Particle-particle response function as a probe for electronic correlations in the *p-d* Hubbard model

S. Ugenti,[1] M. Cini,[1,2] G. Seibold,[3] J. Lorenzana,[4] E. Perfetto,[1,2] and G. Stefanucci[1,2]
[1]*Dipartimento di Fisica, Università di Roma Tor Vergata, Via della Ricerca Scientifica 1, I-00133 Rome, Italy*
[2]*Laboratori Nazionali di Frascati, Istituto Nazionale di Fisica Nucleare, Via E. Fermi 40, 00044 Frascati, Italy*
[3]*Institut für Physik, BTU Cottbus, P.O. Box 101344, 03013 Cottbus, Germany*
[4]*ISC-CNR, Dipartimento di Fisica, Sapienza Università di Roma, Piazzale Aldo Moro 2, I-00185 Rome, Italy*
(Received 4 June 2010; published 27 August 2010)

We discuss and compare different approximations to the particle-particle response function in the *p-d* (three-band) Hubbard model for the CuO_2 plane of superconducting cuprates. Besides the relevance for understanding the role of correlations in high-T_c superconductors, the interest in the CuO_2 plane is due to the presence of three incompletely filled valence bands. The bare ladder approximation (BLA) was employed long ago in the context of Auger core-valence-valence spectroscopy of late transition metals while the time-dependent (TD) Gutzwiller approximation (GA) is a much more sophisticated and recent development. The validity of both is assessed by comparing with exact-diagonalization results from a finite six-site cluster. We find that for standard parameter sets TDGA and BLA yield two-hole spectra in excellent agreement with the exact ones. Although the interaction is comparable to the kinetic energy, the system is far from the extreme Mott limit often assumed in cuprates, where the Mott insulating character is completely local. In order to identify possible fingerprints of the extreme Mott regime we artificially reduce the bandwidth. We find that the BLA breaks down while the TDGA keeps near the exact results. Our findings provide a simple criterion to identify doped and undoped extreme Mott insulators.

DOI: 10.1103/PhysRevB.82.075137 PACS number(s): 71.10.Fd, 82.80.Pv

I. INTRODUCTION

In order to characterize the properties of strongly correlated electron systems, a knowledge of the two-body Green's function is crucial. It is hardly necessary to recall[1] that it appears in the equation of motion of the one-body Green's function and determines the electron self-energy through the scattering amplitude. The two-body Green's function with two pairs of equal times, $P(t-t')$, is known as the particle-particle response function and it contains more direct information on the strength of the electron interaction than any one-body quantity. This can be seen in the dilute limit of the Hubbard model. When the on-site repulsion U is much larger than the bandwidth, the Fourier transform $P(\omega)$ has sharp resonances, or antibound pair states, at energy U above the continuum. These resonances appear in the Auger spectra of closed-shell systems (or hole diluted systems) and allow for a direct determination of the strength of the Coulomb interaction.[2,3] While one would expect Auger spectroscopy to be an ideal tool for the determination of the strength of Coulomb interactions in dense systems too, one obstacle for a widespread use has been the lack of an adequate understanding of the two-body Green's functions itself. This problem has currently become of great interest in superconducting cuprates because the standard classification of cuprates as doped Mott insulators[4] due to a strong local Coulomb interaction has been put into question.[5]

The response function can be computed exactly in the case of two holes added to a closed-shell system and related to their Auger spectra, as shown by Cini and Sawatzky.[2,3] For nearly filled systems the bare ladder approximation (BLA) has been proposed long ago[6] and validated in several cases while the time-dependent Gutzwiller approximation (TDGA) is a recent proposal which has clarified the role of the proximity to a Mott insulating phase in the two-body correlation of dense systems.[7,8]

Cuprates are particularly "simple" transition metals in the sense that only a hybridized band of mainly Cu $d_{x^2-y^2}$ and oxygen $p_{x/y}$ orbitals crosses the Fermi energy. In the electronic structure of the corresponding three-band Hamiltonian a band with mainly Cu character is separated by the charge-transfer gap Δ from the oxygen bands. In the present paper we compare the BLA approximations and the TDGA and assess their respective merits, generalizing the previous one-band results in the more realistic context of the three-band model. The validity of both approaches is checked from a comparison with exact-diagonalization results for a finite cluster.

We show that for the realistic parameter sets used in the literature[9,10] the resulting two-hole spectra are rather similar for BLA and TDGA, indicating that the underlying ground states are not in a "extreme" or "pure" Mott limit defined below. We also use parameter sets in the extreme Mott limit where we find significant differences between both approaches. This provides a simple criterion to decide the Mott character of a given doped or undoped insulator.

Here we use the term "extreme Mott" insulator to specify a Mott insulator in which the insulating character is solely due to the local physics, i.e., does not need antiferromagnetic (AF) correlations as in a Slater picture.[11] We prefer to use the adjective extreme because it is hard to make a sharp distinction between Slater and Mott insulators since at intermediate interaction strengths the two mechanisms can cooperate. To see this consider a half-filled single-band Hubbard model on a bipartite lattice with interaction strength close but below the critical value U_c of a pure Mott transition,[11] i.e., a metal-insulator transition in which all magnetic correlations have been suppressed. Allowing for an AF state, simple estimates

show that one finds an insulator with a gap of order U rather than the AF interaction. Suppressing AF correlations instead the system is metallic. Clearly the Mott and the Slater effects cooperate. It is custom to call a correlated insulator with a gap of order U a Mott insulator, which justifies the use of the adjective extreme or pure for the insulator above U_c. The same concept applies to the three-band Hubbard model in the charge-transfer regime[4,12] with the charge-transfer energy Δ playing the role of an effective U.

It was proposed early on by Anderson that upon doping superconductivity evolves from the correlated insulating state and the single-band Hubbard model was considered adequate for its description. Indeed it is generally believed that at sufficiently low energies, the three-band model can be mapped onto a one-band model with an effective on-site repulsion $U \sim \Delta$. It is still under debate what is the limit of validity of this mapping. We will show below that the mapping does not hold at the energies relevant for Auger spectroscopy.

The paper is organized as follows. In Sec. II we briefly review the relevance of the two-body response to Auger spectroscopy and the theoretical state of the art. In Sec. III we present the model and the approximations used throughout the paper. In Sec. IV we present the approximate results and the comparison with exact diagonalization and finally we conclude in Sec. V.

II. RELEVANCE TO AUGER SPECTROSCOPY

The core-valence-valence (CVV) Auger spectroscopy offers a unique opportunity to observe the two-hole local density of states (LDOS) of the two interacting final-state holes for completely filled bands, such as the d band of Cu Ag or Au. In a CVV Auger process an incoming photon produces a core hole that is subsequently filled by a valence-band electron. The excess energy is transferred to a second (Auger) electron, that is ejected from the sample leaving the system in a two hole state. Studying the energy distribution of the Auger electrons one can obtain information on the excitations of the system with two electrons removed from the valence band. Neglecting interactions the Auger spectra would consist of a continuum given by the self-convolution of the single-hole LDOS.[13] Instead, real spectra in strongly correlated systems, such as transition metals, considerably differ and have an atomiclike character. This was explained by Cini[2] and by Sawatzky[3] who studied the problem of two holes in an otherwise full band described by the Hubbard model. In this extremely dilute hole limit the problem is exactly solvable.

The effect of a large Hubbard on-site interaction U is to split-off a two-hole resonance from the continuum, which is an antibound state. The line shape is very sensitive to the on-site Coulomb energy to bandwidth ratio U/W, making the Auger spectroscopy, in principle, an ideal technique to determine its strength. Using atomic Auger matrix elements, and accounting for multiplet effects, relativistic corrections, crystal field, and some minor corrections, the theory reproduces well the detailed spectral shapes in several cases,[14–16] with a single adjustable repulsion parameter. Recently a successful *ab initio* calculation[17] of the Zn and Cu spectrum was reported.

However, the Auger spectra from incompletely filled bands tend to be disappointingly broad, smooth, and featureless even in magnetic materials where correlations are obviously important. The reason is that the polarizable open band with its continuum of excitations coupled to the core hole produces a superposition of spectra arising from several orthogonal many-body states with a core hole. Moreover, the two final-state holes propagate in the excited valence background and interact with the screening cloud, thus the two-hole-one-electron continuum comes into play. Very sharp structures cannot arise since any two-hole resonances have efficient intraband decay channels and broaden. On top of this, the open-bands theory must account for the quantum coherence between hole creation and decay (the so-called one-step model, see, e.g., Refs. 16 and 18–20). Nevertheless, *unrelaxed* spectral features still exist.[21] These can be assigned to the two-hole states and calculated with $P(\omega)$. On the other hand, a spectacular cleanup of the spectral profile can be achieved by important experimental refinements such as Auger-photoelectron coincidence spectroscopy (APECS),[22] where rather sharp details can again be seen.[23]

Relaxation-induced structures are minor when the bands are almost completely filled and the main effects are captured[16] by a theory[24] in which the equilibrium density of holes (filling) is the small parameter. The response function P is worked out[6,25,26] by a diagrammatic analysis inspired by the T-matrix approximation by Galitzki[27] and its extensions.[28] This approximation consists in performing a ladder resummation using Hartree-Fock (HF) Green's function and we will refer to it as BLA. The more sophisticated self-consistent dressing of the Green's function with the T-matrix self-energy failed to improve over the BLA at larger repulsion and larger hole filling. The reason why the BLA works better is that the error due to the neglect of the dressing of the Green's function tends to cancel with the error due to the neglect of vertex corrections in accord to what is found in other contexts.[29]

The BLA is remarkably successful in cases such as Ni and Pd.[25] However, if the hole filling and the interaction strength are increased, eventually the BLA breaks down.

In recent years two of us have shown[7,8] that the TDGA can overcome the difficulties of the BLA resulting in two-particle spectra in excellent agreement with exact-diagonalization results also for partially filled bands and strong interaction. The TDGA approximation takes into account both the renormalization of the quasiparticle bands due to correlations and the vertex corrections through an effective interactions among quasiparticles. These vertex corrections are crucial close to a Mott insulating state. These results, however, were limited to the one-band Hubbard model and here we consider the extension to the three-band model as usually applied to the cuprates.

We cannot yet afford a comparison with experiments since only early measurements are available[30–32] and they resulted in broad Auger line shapes with no signatures of sharp two holes features. APECS data are probably needed to have the necessary details. Furthermore, the calculation of the relaxed part of the spectrum is, at present, numerically

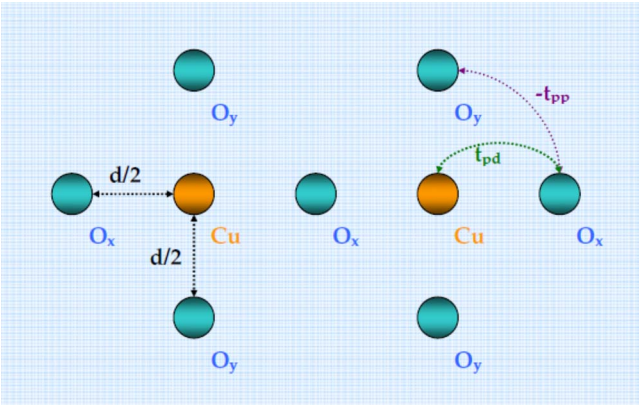

FIG. 1. (Color online) Schematic representation of the atoms arrangement in the considered cluster for CuO_2 planes. As it can be seen from the figure the nearest-neighbors distance between copper and oxygen is always $d/2$ both in the x and in the y directions.

too demanding and hence it cannot be carried out unless reliable approximations are proposed. We here address important preliminary questions: which is the best approximation for the response function, how far we can rely on it, and how the proximity to a Mott insulator state affects the results. We emphasize that the response function is of interest in itself since, as we shall show, it provides significant insight on the Mott transition[7] in the three-band model.

III. MODEL AND APPROXIMATION SCHEMES TO THE RESPONSE FUNCTION

We consider the CuO_2 plane with a single orbital per atom, i.e., the $d_{x^2-y^2}$ orbital for copper and a p orbital for oxygen. Within each primitive cell, the two oxygen atoms have been labeled as O_x and O_y according to their position with respect to the Cu atom, as shown in Fig. 1. The distance between the Cu and O atoms is $d/2$ with d the lattice spacing. With one orbital per atom we expect three energy bands. In the parent compound two of them are fully occupied by electrons while the remaining one is half filled.

We introduce the creation (annihilation) operators $c_{i\sigma}$ ($c_{i\sigma}^\dagger$) of holes at site i with spin σ. The Hamiltonian of the system is taken of the Hubbard-type form,

$$H = H_0 + H_1 \tag{1}$$

with the one-particle part,

$$H_0 = \sum_{i\sigma} \varepsilon_i c_{i\sigma}^\dagger c_{i\sigma} + \sum_{i\neq j\sigma} t_{ij} c_{i\sigma}^\dagger c_{j\sigma}, \tag{2}$$

where $\varepsilon_i = \varepsilon_d, \varepsilon_p$ for a Cu or a O, respectively. The hopping $t_{ij} = t_{pd}$ for nearest-neighbor Cu-O and $t_{ij} = t_{pp}$ for nearest-neighbor O-O. The on-site repulsive interaction is modeled as

$$H_1 = \sum_i U_i n_{i\uparrow} n_{i\downarrow} \tag{3}$$

with $U_i = U_d, U_p$ for a Cu or an O, respectively. In Eq. (3) the operator $n_{i\sigma} \equiv c_{i\sigma}^\dagger c_{i\sigma}$ is the number operator for a hole at site i with spin σ. For simplicity interatomic interactions are neglected.

Our aim is to compute the response function

$$P^{ij}(t) = \frac{1}{i}\langle \Phi_N^{(0)} | \mathcal{T}\{c_{i\uparrow}(t) c_{i\downarrow}(t) c_{j\downarrow}^\dagger c_{j\uparrow}^\dagger\} | \Phi_N^{(0)} \rangle, \tag{4}$$

where $i = (\alpha, m)$ is a collective index that labels an $\alpha = p_x, p_y, d$ atom in the mth cell. We will use the notation $P^{ij} = P_{mn}^{\alpha\beta}$ when the explicit form of the collective indices is needed. In Eq. (4), $|\Phi_N^{(0)}\rangle$ is the system ground state with N holes, $\mathcal{T}$ represents the time-ordered product, and $c(t)$ are the hole operators in the Heisenberg picture. In the ω space the response function can be expressed using the Lehmann representation as

$$P^{ij}(\omega) = \sum_\nu \frac{A_\nu(i) A_\nu^*(j)}{\omega + (E_{N-2}^{(\nu)} - E_N^{(0)}) - i\delta} - \sum_\nu \frac{B_\nu^*(i) B_\nu(j)}{\omega + (E_N^{(0)} - E_{N+2}^{(\nu)}) + i\delta}$$

with

$$A_\nu = \langle \Phi_N^{(0)} | c_{j\downarrow}^\dagger c_{j\uparrow}^\dagger | \Phi_{N-2}^{(\nu)} \rangle, \quad B_\nu = \langle \Phi_{N+2}^{(\nu)} | c_{j\downarrow}^\dagger c_{j\uparrow}^\dagger | \Phi_N^{(0)} \rangle. \tag{5}$$

Here, the states $|\Phi_M^{(\nu)}\rangle$ are eigenstates of the Hamiltonian H with M holes and energy $E_M^{(\nu)}$.

A. Cini-Sawatzky theory and bare ladder approximation

We start considering the case of completely filled bands. Then, the addition part in Eq. (5) vanishes and the response function becomes

$$P^{ij}(\omega) = \langle 0 | c_{i\uparrow} c_{i\downarrow} \frac{1}{\omega - H + i\delta} c_{j\downarrow}^\dagger c_{j\uparrow}^\dagger | 0 \rangle \tag{6}$$

with $|0\rangle = |\Phi_0^{(0)}\rangle$ the hole vacuum ket. Using the Dyson equation

$$\frac{1}{\omega - H + i\delta} = \frac{1}{\omega - H_0 + i\delta} + \frac{1}{\omega - H_0 + i\delta} H_1 \frac{1}{\omega - H + i\delta}, \tag{7}$$

we can easily obtain a system of coupled equations which allows us to build $P(\omega)$ in terms of the noninteracting response function $P^0(\omega)$. As an example we can build the Cu-Cu matrix element $P_{mn}^{dd}(\omega)$,

$$P_{mn}^{dd}(\omega) = P_{mn}^{0,dd}(\omega) + \sum_{\alpha = d, p_x, p_y} U_\alpha \sum_s P_{ms}^{0,d\alpha}(\omega) P_{sn}^{\alpha d}(\omega), \tag{8}$$

where the s sum runs over the cells of the two-dimensional lattice. In a similar manner we can write an equation for the Cu-O and O-O matrix elements of the response function. Using a matrix notation in the $\{dd, p_x p_x, p_y p_y\}$ space, the total system of coupled equations can be represented as

$$\hat{P}_{mn}(\omega) = \hat{P}_{mn}^0(\omega) + \sum_s \hat{P}_{ms}^0(\omega) \hat{U} \hat{P}_{sn}(\omega), \tag{9}$$

where the Coulomb matrix $\hat{U}$ is defined according to

$$\hat{U} \equiv \begin{pmatrix} U_d & 0 & 0 \\ 0 & U_p & 0 \\ 0 & 0 & U_p \end{pmatrix}. \tag{10}$$

Following Sawatzky,[3] Eq. (8) decouples in the basis of delocalized Bloch states with momentum $\mathbf{q}$, and the problem reduces to the solution of a 3×3 linear system. Denoting by $\hat{P}_{\mathbf{q}}(\omega)$ the Fourier transform of the response function in $\mathbf{q}$ space it is straightforward to show that

$$\hat{P}_{\mathbf{q}}(\omega) = [\hat{I} - \hat{P}^0_{\mathbf{q}}(\omega)\hat{U}]^{-1}\hat{P}^0_{\mathbf{q}}(\omega), \tag{11}$$

where $\hat{I}$ is the identity matrix. The desired local response is obtained as

$$P^{\alpha\alpha}_{\mathrm{loc}}(\omega) \equiv P^{\alpha\alpha}_{mm} = \frac{1}{\Omega}\sum_{\mathbf{q}} P^{\alpha\alpha}_{\mathbf{q}}(\omega)$$

with Ω the number of unit cells in the system. We also define the total response

$$P_{\mathrm{tot}}(\omega) = \sum_{\alpha} P^{\alpha\alpha}_{\mathrm{loc}}(\omega).$$

At finite filling the above result is no longer exact since the two holes can interact with the background holes as well. In the dilute limit (low filling) an excellent approximation is to compute the response by summing a ladder series with Hartree-Fock (bare) propagators leading to the BLA. The result can be obtained from Eq. (11) by replacing the (zeroth-order) Green's function in P^0 by the HF Green's function, i.e., the Green's function of the HF Hamiltonian (see Appendix),

$$H_{\mathrm{HF}} = \sum_{i\sigma} (\varepsilon_i + \Sigma^{\mathrm{HF}}_i) c^\dagger_{i\sigma} c_{i\sigma} + \sum_{i\neq j\sigma} t_{ij} c^\dagger_{i\sigma} c_{j\sigma}. \tag{12}$$

For Hubbard-type interactions the (spin-compensated) HF self-energy is simply

$$\Sigma^{\mathrm{HF}}_i = U_i \langle n_i\rangle/2 \tag{13}$$

with $\langle n_i\rangle$ the average occupation number in the hole picture of the ith atom ($n_i \equiv \Sigma_\sigma n_{i\sigma}$).

B. Time-dependent Gutzwiller approximation

The derivation of the TDGA equation in the p-d Hubbard model is a straightforward generalization of the derivation presented in Refs. 7 and 8 for the single-band Hubbard model and it is briefly sketched below.

The starting point is the Gutzwiller wave function[33–35] that is defined according to

$$|\Phi\rangle = \hat{P}_g |\phi\rangle,$$

where $\hat{P}_g$ partially projects out doubly occupied sites from the state $|\phi\rangle$. We assume $|\phi\rangle$ to be a BCS state since the response function P can be thought of as the response to a time-dependent pairing field which induces time-dependent pairing correlations. This variational freedom is necessary to calculate P but the actual ground state will be nonsuperconducting.

We define the uncorrelated single-particle density matrix $\rho_{i\sigma j\sigma'} \equiv \langle\phi| c^\dagger_{j\sigma'} c_{i\sigma}|\phi\rangle$ and the pair matrix $\kappa_{i\sigma,j\sigma'} \equiv \langle\phi| c_{j\sigma'} c_{i\sigma}|\phi\rangle$, which satisfy the following constraints:[36]

$$\rho^2 - \rho = \kappa\kappa^*, \quad [\rho,\kappa] = 0. \tag{14}$$

All the quantities ρ and κ are assumed to be time dependent due to the action of the pairing field.

The first step is to construct the charge rotationally invariant energy functional $E \equiv \langle\Phi|H|\Phi\rangle$ in the GA. This is more easily done by rotating at each site the fermion annihilation and creation operators to a basis where the anomalous expectation values vanish.[37] Then, one derives the GA with one of the known techniques[38,39] and rotates back to the original operators. Restricting to a nonmagnetic state, $\rho_{i\uparrow j\uparrow} = \rho_{i\downarrow j\downarrow}$, one finds

$$E[\rho,\kappa,D] = \sum_{i\sigma} \varepsilon_i \rho_{ii\sigma} + \sum_{i\neq j\sigma} t_{ij} z_i z_j \rho_{ji\sigma} + \sum_i U_i D_i \tag{15}$$

with $\rho_{ij\sigma} \equiv \rho_{i\sigma,j\sigma}$ and with the hopping renormalization factors,

$$z_i = \frac{\sqrt{\frac{1}{2} - D_i + J_{iz}}\left(\sqrt{D_i - J_{iz} - J_i} + \sqrt{D_i - J_{iz} + J_i}\right)}{\sqrt{\frac{1}{4} - J_i^2}}. \tag{16}$$

Here we defined

$$J_{ix} = \frac{1}{2}(\kappa_{i\uparrow,i\downarrow} + \kappa^*_{i\uparrow,i\downarrow}),$$

$$J_{iy} = \frac{i}{2}(\kappa_{i\uparrow,i\downarrow} - \kappa^*_{i\uparrow,i\downarrow}),$$

$$J_{iz} = \frac{1}{2}(\rho_{i\uparrow,i\uparrow} + \rho_{i\downarrow,i\downarrow} - 1),$$

$$J_i \equiv |\mathbf{J}_i|, \tag{17}$$

and the double occupancy

$$D_i = \langle\Phi| n_{i\uparrow} n_{i\downarrow}|\Phi\rangle.$$

The ground state is found by minimizing Eq. (15) with the constraints, Eq. (14), leading to the static ρ^0, κ^0, $\mathbf{J}^0$, and D^0. (We use the nought to indicate quantities evaluated at the minimum.) We will consider a paramagnetic normal metal thus $\kappa^0 = J^0_x = J^0_y = 0$ and

$$z^0_i = \frac{\sqrt{(\rho^0_{ii\sigma} - D^0_i)(1 - \rho^0_{ii} + D^0_i)} + \sqrt{D^0_i(\rho^0_{ii\bar{\sigma}} - D^0_i)}}{\rho^0_{ii\sigma}(1 - \rho^0_{ii\sigma})}, \tag{18}$$

where we defined the total density on site i as $\rho_{ii} = \Sigma_\sigma \rho_{ii\sigma} = 2\rho_{ii\uparrow} = 2\rho_{ii\downarrow}$. It is useful to define the Gutzwiller quasiparticle Hamiltonian at the minimum,

$$H_{\mathrm{GA}} = \sum_{ij\sigma} \left.\frac{\partial E}{\partial \rho_{ji\sigma}}\right|_{\rho^0} c^\dagger_{i\sigma} c_{j\sigma}$$
$$= \sum_{i\sigma} (\varepsilon_i + \Sigma^{\mathrm{GA}}_i) c^\dagger_{i\sigma} c_{i\sigma} + \sum_{i\neq j\sigma} t_{ij} z^0_i z^0_j c^\dagger_{i\sigma} c_{j\sigma}, \tag{19}$$

where the local Gutzwiller self-energy is

$$\Sigma_i^{\mathrm{GA}} = \left.\frac{\partial E}{\partial \rho_{ii\sigma}}\right|_{\rho^0} - \varepsilon_i \tag{20}$$

and coincides with the Lagrange parameter of the slave boson method.[38]

To compute the response function we add a weak time-dependent pairing field

$$F(t) = \sum_i (f_i e^{-i\omega t} c_{i\downarrow} c_{i\uparrow} + \mathrm{H.c.})$$

to the Hamiltonian in Eq. (1). This produces small time-dependent deviations $\delta\rho(t) = \rho(t) - \rho^0$. In addition, since F does not conserve the particle number, it induces pairing correlations κ, which we compute in linear response.

Previously,[34,35,40] the energy was expanded to second order in terms of particle-hole fluctuations, leading to effective matrix elements for charge and spin excitations. For a normal paramagnet neither those channels nor δD fluctuations mix with the particle-particle channel, thus simplifying the formalism. The remaining part follows text book computations in nuclear physics.[36] Expanding the energy up to second order in $\delta\rho$ and κ one finds

$$\delta E = \sum_{\mathbf{k}\nu\sigma} \varepsilon_{\mathbf{k}\nu} \delta\rho_{\mathbf{k}\nu\sigma} + \sum_i V_i (J_{ix}^2 + J_{iy}^2). \tag{21}$$

Here $\varepsilon_{\mathbf{k}\nu}$ denotes the GA dispersion relation obtained by diagonalizing the GA Hamiltonian (19). The effective on-site particle-particle interaction is

$$V_i = \frac{U_i - 2\Sigma_i^{\mathrm{GA}}}{1 - \langle n_i \rangle}. \tag{22}$$

The response function can be readily derived from the equations of motion of the pair matrix in a normal system after using the constraint, Eq. (14), to express the first term in Eq. (21) as a quadratic contribution in κ.[36] The pair-correlation function is given by the same ladder expression (11) of the BLA but with the zeroth-order Green's function replaced by time-ordered Green's function of the GA Hamiltonian (see Appendix) and the effective interaction,

$$\hat{U} \equiv \begin{pmatrix} V_d & 0 & 0 \\ 0 & V_p & 0 \\ 0 & 0 & V_p \end{pmatrix}. \tag{23}$$

IV. RESULTS

A. General structure of the spectra

The two-hole LDOS of copper and oxygen [see Secs. IV B and IV C] can be obtained from the imaginary part of $\hat{P}_{\mathrm{loc}}(\omega)$. This can be calculated from Eqs. (11) and (A5) for both BLA and GA. The results given by these two methods differ one from the other because of the different way BLA and GA introduce and treat electronic correlations. The BLA introduces correlation effects only through the Coulomb matrix $\hat{U}$, so the diagram for $\hat{P}_{\mathbf{q}}^0$ shows a pair of HF Green's function. In the Gutzwiller approach, instead, electronic correlations are present not only in $\hat{U}$, but also in $\hat{P}_{\mathbf{q}}^0$ by means of the renormalized hopping parameters and on-site energies. In addition, the bare Hubbard repulsion parameters in $\hat{U}$ are replaced by the effective V_α, see Eq. (23), which contains vertex corrections. It is interesting to notice that Eq. (22) is a general expression returning, for a given approximation scheme, the effective interaction consistent with that approximation. As an example by replacing Σ_i^{GA} with the Hartree-Fock self-energy, we obtain the bare Coulomb parameters entering the BLA.

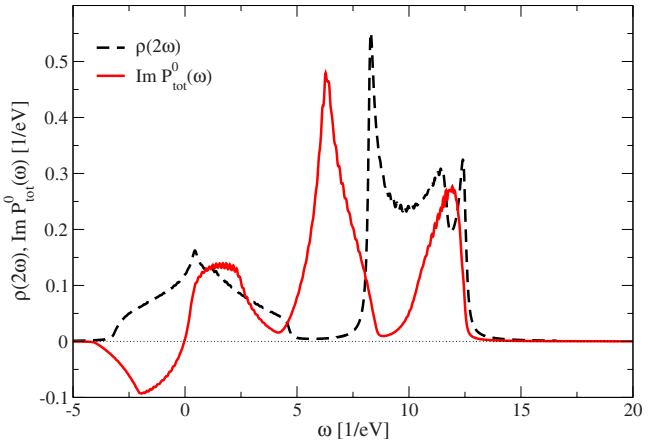

FIG. 2. (Color online) Single-hole DOS $\rho(\omega/2)$ (dashed) and noninteracting two-hole DOS (red solid) for the three-band Hubbard model computed within the GA. For the single-hole DOS the energy has been scaled by a factor of 2 to make one-body features overlap with the corresponding two-body structures.

The results presented in this section are for the cuprate parameters taken from Ref. 9, i.e., $t_{pd}=1.6$ eV, $t_{pp}=-0.6$ eV, $\Delta \equiv \varepsilon_p - \varepsilon_d = 2.75$ eV, $U_p=3.6$ eV, and $U_d=7.9$ eV. In the following we will refer to this set of parameters as the "physical parameter set." To address the spectra closer to the Mott transition we will also consider smaller values of the hopping amplitudes t_{pd} and t_{pp}.

In Fig. 2 we show the general structure of the single-hole DOS and the two-hole DOS for the three-band Hubbard model, both computed by the GA including z_i and Σ_i^{GA} but excluding hole-hole interactions. We have evaluated the single-hole DOS at $\omega/2$ so as to have an overlap between the one-body and the two-body excitations. Here the two-hole noninteracting DOS corresponds to the trace of the imaginary part of Eq. (A5) summed over all momenta $\mathbf{q}$. The one-hole DOS is composed of two bands where the lower (upper) one has mainly contributions from copper (oxygen) states. The two-hole DOS shows three-bands with copper-copper, copper-oxygen, and oxygen-oxygen excitations. A positive (negative) sign corresponds to particle addition (removal) so that Im P_{tot}^0 changes sign at $\omega - 2E_F = 0$ with E_F the Fermi energy.

For the system under consideration we have one hole per copper so that the lower band in the one-hole DOS is half filled (the zero of the energy axis references the Fermi energy). Notice that copper oxides are insulating at half filling while we are considering a metal. It is legitimate to ask if one can incorporate this behavior in the bare Green's func-

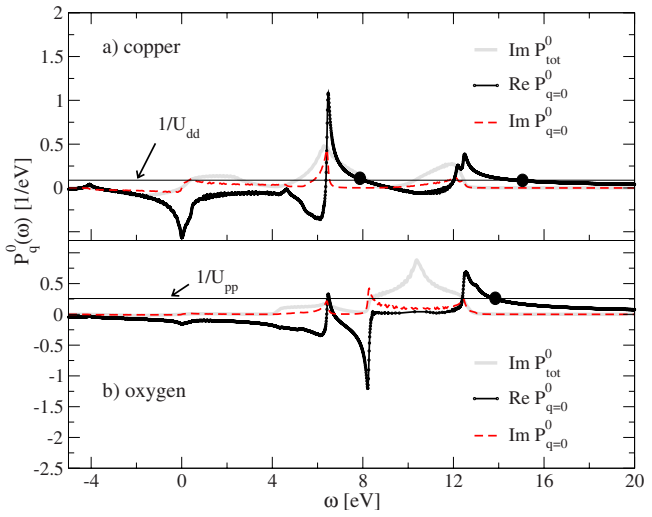

FIG. 3. (Color online) Uncorrelated two-particle Green's function $P^{0,\alpha\alpha}_{\mathbf{q}}(\omega)$ for (a) copper and (b) oxygen. Thick gray line: imaginary part summed over all momenta. Solid and dashed: real and imaginary part for momentum $\mathbf{q}=(0,0)$. The horizontal lines show the inverse of the local interactions which cut the real parts at energies marked with a solid dot.

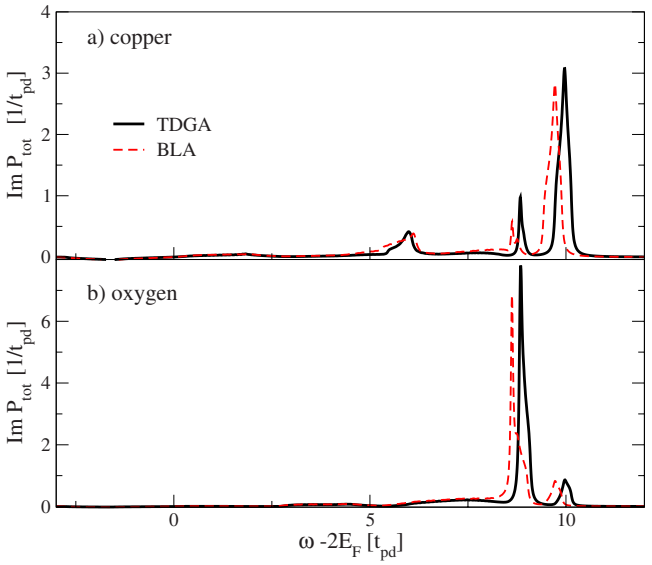

FIG. 4. (Color online) Imaginary part of the response function $P^{\alpha\alpha}_{\mathrm{loc}}(\omega)$ for copper and oxygen within TDGA (solid) and BLA (dashed) at band filling $n=1$. The parameters are the physical parameter set from Ref. 9: $t_{pd}=1.6$ eV, $t_{pp}=-0.6$ eV, $\Delta=2.75$ eV, $U_p=3.6$ eV, $U_d=7.9$ eV, and filling $n=1$.

tion. We will see below that for realistic parameters the GA approximation does not predict a paramagnetic correlated insulating state at half filling, although such state is possible. This already points to a situation in which the system is not in the extreme Mott limit. We can reproduce the insulating behavior, of course, by extending the variational freedom of the Gutzwiller wave function to have AF order (not shown). For simplicity we will restrict to paramagnetic states so our results are strictly valid away form half filling where the ground state is paramagnetic.

Upon the inclusion of Coulomb interactions the new poles of the response function are determined by Eq. (11). When, in a first step, we ignore the off-diagonal elements of $P^{0,\alpha\beta}_{\mathbf{q}}(\omega)$ (i.e., $\alpha\neq\beta$) then the poles of $P^{\alpha\alpha}_{\mathbf{q}}(\omega)$ are determined from $1-U_\alpha P^{0,\alpha\alpha}_{\mathbf{q}}(\omega)=0$ in the BLA approximation and $1-V_\alpha P^{0,\alpha\alpha}_{\mathbf{q}}(\omega)=0$ in the TDGA. This is exemplified in Fig. 3 which for both copper and oxygen displays the real and imaginary part of $P^{0,\alpha\alpha}_{\mathbf{q}}(\omega)$ for momentum $\mathbf{q}=(0,0)$ together with the inverse of the Hubbard repulsion parameters. The dominant (undamped) excitations appear at energies for which $\mathrm{Re}\,P^{0,\alpha\alpha}_{\mathbf{q}}(\omega)=1/U_\alpha$ and $\mathrm{Im}\,P^{0,\alpha\alpha}_{\mathbf{q}}(\omega)=0$; in Fig. 3 these energies are indicated by a solid dot. Note that the lower energy pole (at $\omega\approx 8$ eV) in the Cu LDOS is undamped only for $\mathbf{q}=(0,0)$. In fact, the total two-hole LDOS is finite at this energy (thick gray line) and hence damping for other momenta must be present.

In a single-band picture the lower band is described by a one-band Hubbard model with an effective interaction U_{eff}. The values of U_{eff} are such as to generate a two-hole antibound state in the spectrum. It is interesting to observe that our results in the three-band model show that no single poles can be associated with the lower band. This is because the putative resonance overlaps with the continuum of states in which one hole is on the Cu band and one hole is on the O band. Therefore it is already clear from this figure that the single-band picture does not apply at the energies relevant for Auger spectroscopy. For the same parameters, Fig. 3 will only change little when the system is treated within the TDGA. (Instead if the bandwidth is strongly reduced to drive the system into an extreme Mott regime strong differences between BLA and TDGA arise as it will be shown in Sec. IV C.)

Taking also into account the off-diagonal elements $P^{0,\alpha\beta}_{\mathbf{q}}(\omega)$ in the solution of Eq. (11) will induce a mixing $\sim t_{pd}$ between Cu and O spectra. For the local response function $P^{\alpha\alpha}_{\mathrm{loc}}(\omega)$ we therefore expect three features related to the two copper and one oxygen excitation as discussed above.

B. Results for the physical parameter set

We define the filling n as the number of holes per Cu site. Figure 4 shows $\mathrm{Im}\,P^{\alpha\alpha}_{\mathrm{loc}}(\omega)$ for both copper and oxygen computed for a half-filled system ($n=1$) and the physical parameter set. As anticipated before the copper LDOS displays three main features, one of which (at $\omega\approx 13$ eV) arises due to the coupling with the oxygen two-hole excitations, see top panel. Similarly the Cu feature at $\omega\approx 15$ eV is admixed with the oxygen LDOS. On the contrary, the lower-energy copper band at $\omega\approx 8$ eV is not visible in the oxygen spectrum due to its low weight, see bottom panel. Moreover it turns out that the spectra obtained within the TDGA are not much different from those computed within the BLA except for a slight shift of the high-energy excitations. This shift can be traced back to the different Fermi energies in the GA and HF approximations which determines the location of the peaks relative to $2E_{\mathrm{F}}$. Quite generally one finds that for the same number of particles $E_{\mathrm{F}}^{\mathrm{GA}}<E_{\mathrm{F}}^{\mathrm{HF}}$ since $\Sigma^{\mathrm{GA}}<\Sigma^{\mathrm{HF}}$. This is so because in the GA the holes tend to avoid each other and hence "feel" a reduced Coulomb repulsion (correlation ef-

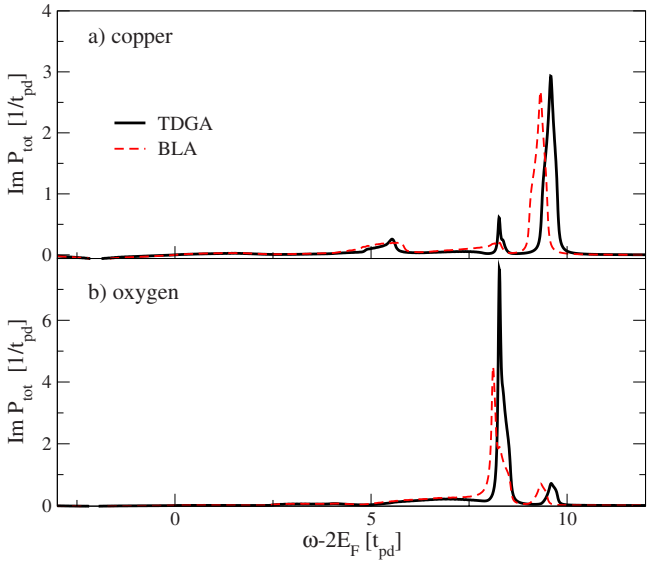

FIG. 5. (Color online) Same as Fig. 4 but for filling $n=1.2$.

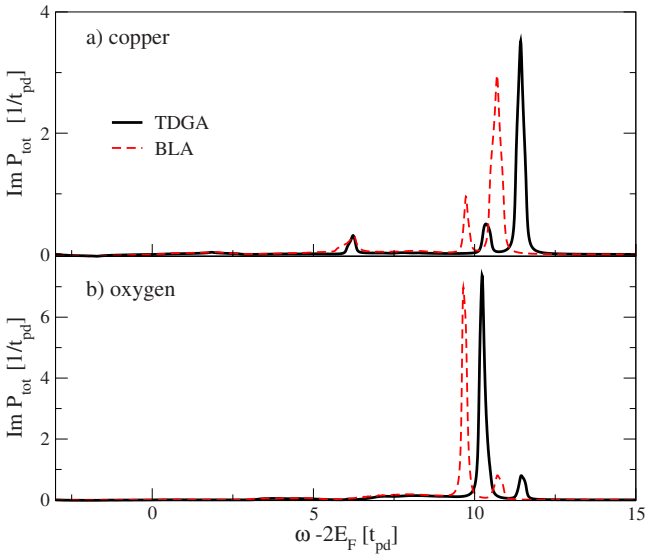

FIG. 6. (Color online) Imaginary part of the response function $P^{\alpha\alpha}_{\mathrm{loc}}(\omega)$ for copper and oxygen within TDGA (solid) and BLA (dashed) at half filling. The parameters are taken from Ref. 10: $t_{pd}=1.3$ eV, $t_{pp}=-0.65$ eV, $\Delta=3.6$ eV, $U_p=4.$ eV, and $U_d=10.5$ eV.

fect). If, on the other hand, we refer the energies to the same origin as that of the parameters of the Hamiltonian, hereafter the "absolute scale," the poles essentially coincide. This implies that the disagreement among the approaches can be traced back to the disagreement in the respective self-energies. This is analogous to what was found in the single-band Hubbard model (see Ref. 7 for a more detailed discussion on this point).

The spectra of the doped system are displayed in Fig. 5. They are quite close to those of the half-filled model except for a slight shift of the dominant excitations to lower energy for both TDGA and BLA. In the absolute scale the poles do not move so the shift can entirely be attributed to the increase in the Fermi energy upon hole doping. The structure of the two-hole LDOS does not differ significantly for the various parameter sets available in the literature. Figure 6 shows the spectra for the undoped system calculated with the parameter set of Ref. 10. The slightly larger shift of the BLA spectrum to lower energies as compared to Fig. 4 is a consequence of the larger difference $E_{\mathrm{F}}^{\mathrm{GA}}-E_{\mathrm{F}}^{\mathrm{HF}}$ caused by the increased ratio U_d/t_{pd}.

C. Results near the extreme Mott limit

The previous results have shown that the inclusion of correlations beyond the BLA has only a marginal influence on the spectra for the "physical parameter set." On the other hand, our previous investigations on the one-band model[7] revealed that the BLA and TDGA spectra are quite distinct close to (or inside) the extreme Mott regime. The differences are mainly reflected in (a) a strong bandwidth renormalization of the TDGA and (b) a different behavior of the onsite self-energies Σ_i^{GA} which, as we shall show, has a large impact on the two-hole excitations.

When the TDGA is applied to the one-band Hubbard model the extreme Mott regime can be identified from the appearance of the Brinkman-Rice metal-insulator[41] transition above the critical $U=U_{BR}$. In the three-band Hubbard model one finds the same physics controlled by the Coulomb repulsion U_d if $\varepsilon_d-\varepsilon_p>U_d$, and by $\varepsilon_d-\varepsilon_p$ otherwise. This has been demonstrated by Balseiro *et al.*[12] using the slave-boson mean-field technique, which can be shown to be equivalent to the GA. In other words, an infinite U_d does not *per se* imply that the system is an insulator; one finds that for infinite U_d and $t_{pp}=U_p=0$ the system is an insulator for $\varepsilon_d-\varepsilon_p>6.2t_{pd}$ while for the finite t_{pp} of Ref. 9 it must be $\varepsilon_d-\varepsilon_p>11t_{pd}\sim 16$ eV. In cuprates the difference $\varepsilon_d-\varepsilon_p$ is about $2t_{pd}$, thus suggesting that these compounds are not extreme Mott insulators.

To study the two-hole response function close to the onset of the extreme Mott insulator regime we artificially reduced all hoppings to 20–25 % of the physical values considered in the previous section. In this case one finds a strong effective reduction in the hopping amplitudes via the Gutzwiller z factors defined in Eq. (18). This in turn induces a significant decoupling of copper and oxygen states. The renormalization of the width of the one-hole energy bands strongly depends on the filling as shown in Fig. 7(a). At half filling the Cu-like band and the chemical potential have a discontinuity due to the presence of the correlation gap. Notice that the Cu-like band becomes of zero width at the transition. Its evolution is similar to the one shown in Fig. 1 of Ref. 7 for the single-band Hubbard model, as expected from the three-band to one-band mapping. For the physical parameters set the evolution is smooth (with no jump) and the band narrowing effect is quite mild (not shown).

In Fig. 7(b) we show the corresponding two-hole bands. According to the three-band to one-band mapping we expect that the holes experience an effective interaction U_{eff} of order $\varepsilon_d-\varepsilon_p$, producing an antibound state halfway between the $n<1$ and $n>1$ Cu-like bands [around 2.2 eV in Fig. 7(b)]. For $n<1$ (electron doping) this antibound state corresponds to the addition of two holes, and is therefore accessible in a

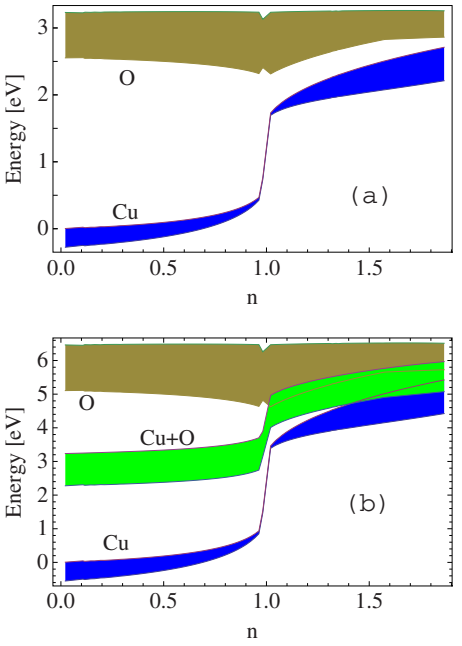

FIG. 7. (Color online) Evolution of the width of the bands versus hole concentration n within the GA. The parameters are $t_{pd}=0.3$ eV, $t_{pp}=-0.12$ eV, $\varepsilon_d-\varepsilon_p=2.75$ eV, $U_p=3.6$ eV, and $U_d=7.9$ eV, and correspond to the extreme Mott limit. In (a) one-hole energy bands are shown; the lower band is the Cu-like band that crosses the Fermi level. (b) displays the two-hole energy bands; the central band is associated to configurations in which one hole is in the Cu-like band and the other is in a O-like band.

Auger decay. However its energy overlaps the Cu+O band and would result in a broad feature. Indeed such resonance will not be seen in any of the spectra displayed below. Again, this shows that the three-band to one-band mapping fails at high energies. For $n>1$ (hole doping) the TDGA in the one-band model correctly predicts an antibound state below the Fermi level whose width vanishes like $1-n$ close to half filling. Below we show that such antibound state appears in the three-band model as well. Notice that this resonance corresponds to two-hole removal and therefore it is not detectable by Auger spectroscopy but would, in principle, be visible in appearance potential spectroscopy.

For completely decoupled bands only the atomiclike resonances survive. Within the TDGA these resonances occur at $\omega\approx 2\varepsilon_p+2\Sigma_p^{\mathrm{GA}}+V_p=2\varepsilon_p+U_p$ for oxygen and $\omega\approx 2\varepsilon_d+U_d$ for copper in the absolute scale. In the present case with a partially filled Cu band and energies referenced to $2E_{\mathrm{F}}$ these excitations occur at $\omega-2E_{\mathrm{F}}\approx U_d-2\Sigma_d^{\mathrm{GA}}$ for Cu and at $\omega-2E_{\mathrm{F}}\approx 2\Delta+U_p-2\Sigma_d^{\mathrm{GA}}$ for O. Figure 8 demonstrates the validity of these arguments for the half-filled system with parameters slightly below the critical ones for the extreme Mott regime. At the minimum the z factors take the value $z_d^0\approx 0.27$ and $z_p^0=1$ leading to an effective Cu-O hopping $z_p^0 z_d^0 t_{pd}$ which is only 6% of the $t_{pd}=1.6$ eV of the physical parameter set. The TDGA self-energy $\Sigma_d^{\mathrm{GA}}\approx 1.1$ eV leads to renormalization of the Cu levels toward the O band and we expect the oxygen antibound state at $2\Delta+U_p-2\Sigma_d^{\mathrm{GA}}\approx 7$ eV which is in fact observed in Fig. 8. On the contrary, the spectral intensity of the copper antibound state is strongly

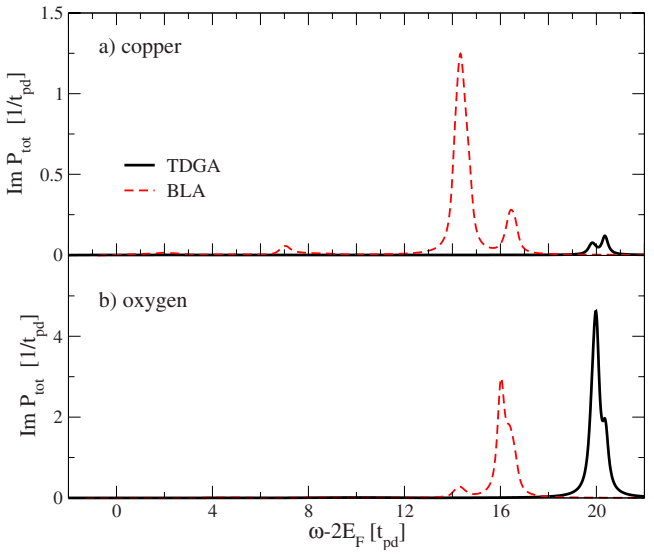

FIG. 8. (Color online) Imaginary part of the response function $P_{\mathrm{loc}}^{\alpha\alpha}(\omega)$ for copper and oxygen within TDGA (solid) and BLA (dashed) at band filling $n=1$. The parameters are: $t_{pd}=0.35$ eV, $t_{pp}=-0.14$ eV, $\varepsilon_d-\varepsilon_p=2.75$ eV, $U_p=3.6$ eV, and $U_d=7.9$ eV.

suppressed due to the vanishing of the Cu double occupancy at half filling upon approaching the extreme Mott phase.[7] The estimate of the position of the peak for completely decoupled copper states ($\omega-2E_{\mathrm{F}}\approx U_d-2\Sigma_d^{\mathrm{GA}}\approx 5.7$ eV) has to be corrected due to the residual hopping which pushes the excitations close to the antibound oxygen state.

Interestingly the closeness to the extreme Mott limit leads to completely different spectra in the case of BLA. In fact, the Cu/O occupancies within the TDGA are $n_d\approx 0.97$, $n_p\approx 0.015$ whereas $n_d\approx 0.6$, $n_p\approx 0.2$ within the BLA, reflecting a still rather delocalized state. As a consequence the energy of both Cu and O excitations is underestimated. Again, this is due to the shift of the Fermi energy to high values caused by $\Sigma_d^{\mathrm{HF}}\gtrsim 2\Sigma_d^{\mathrm{GA}}$ for the present parameters. Figure 9 shows the spectra for the strong-coupling parameter set and

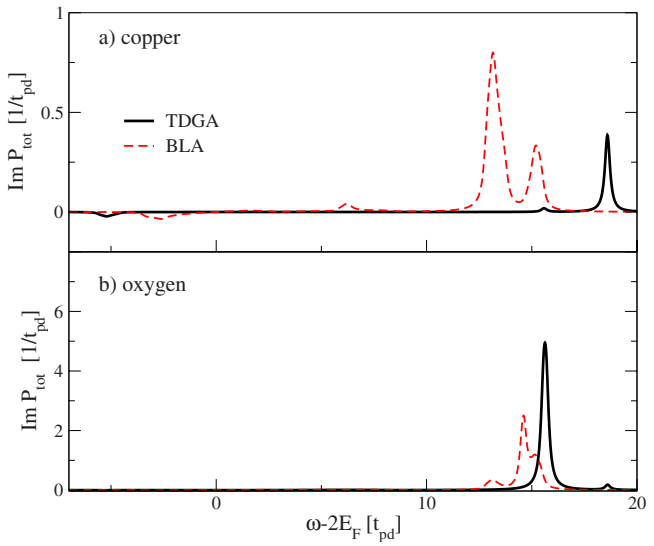

FIG. 9. (Color online) Same as Fig. 8 but for filling $n=1.2$.

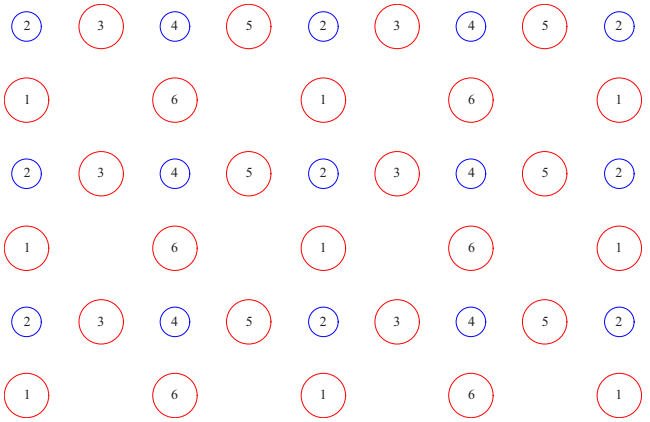

FIG. 10. (Color online) Geometry of the 6-atom cluster with periodic boundary conditions described in the main text. The only k vectors are $(k_x,k_y)=\{(0,0),(\pi,0)\}$. Since atoms 1 and 6 are twice nearest neighbor of 2, 4, respectively, and twice next nearest neighbor of 3 and 5 we took $t_{12}=t_{64}=2t_{pd}$ and $t_{13}=t_{15}=t_{63}=t_{65}=2t_{pp}$.

doping $n=1.2$. Away from half filling the Cu double occupancy increases and so does the weight of the Cu antibound state whose position slightly shifts to lower energy due to the increase in E_F. In addition, the structure that appears at negative energies can be identified with the analog of the one-band antibound state as anticipated above. As compared to half filling the Cu onsite self-energy changes to a value of $\Sigma_d \approx 2$ eV. As a consequence the oxygen antibound state is expected to appear at $2\Delta+U_p-2\Sigma_d \approx 5.1$ eV, close to the value observed in Fig. 9.

A fingerprint of the strong correlations is the relative weight w_r between the oxygen and copper two-hole resonances in the LDOS. For the physical parameter set these weights are approximately equal for both the BLA and the TDGA. Nevertheless, at half filling and approaching the Brinkman-Rice transition, the TDGA predicts a vanishingly small weight of the Cu antibound state while the BLA yields a much larger value. For doping $n=1.2$ (cf. Fig. 9) the ratio between the weight is $w_r \approx 20$ within the TDGA.

D. Comparisons with exact results from a finite cluster

In order to test the validity of our results we compare both the BLA and TDGA against exact results from a finite cluster. We considered the six-site cluster of Fig. 10 with periodic boundary conditions. The only **k** vectors are $(k_x,k_y)=\{(0,0),(\pi,0)\}$. Note that spectra for oxygen(1) and oxygen(3) in general are not identical since the latter couples to two different Cu atoms whereas the former is connected by the periodic boundary conditions to the same Cu atom. Increasing the cluster size the number of configuration grows extremely fast and the small cluster used here is already sufficient for a qualitative comparison between the various approaches.

Figure 11 shows a comparison between exact results, TDGA, and BLA for the half-filled cluster (i.e. one spin-up and one spin-down holes) and the physical parameter set. Here, energies are not referenced to the Fermi energy. We find essentially the same structure of the spectra as in Fig. 4

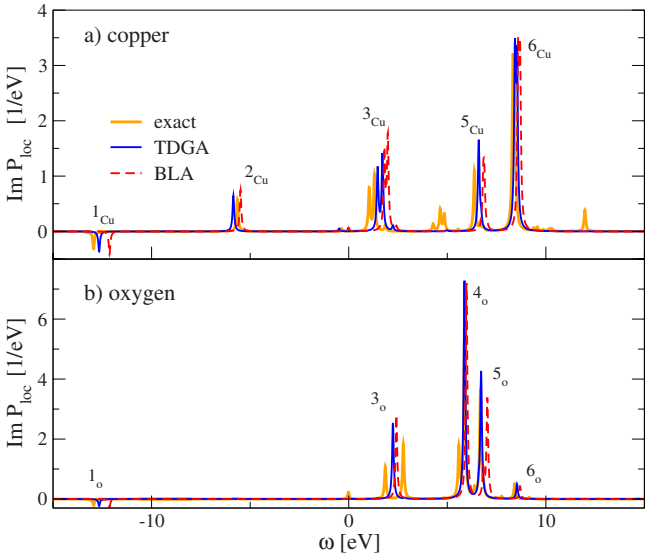

FIG. 11. (Color online) Comparison of the imaginary part of the response function for (a) copper and (b) oxygen between exact (thick solid), TDGA (thin solid), and BLA (thin dashed). The system is a half-filled cluster ($n=1$) and the spectra for oxygen(2) and oxygen(3) are identical. Peak labels are explained in the text. Parameters: $t_{pd}=1.6$ eV, $t_{pp}=-0.6$ eV, $\Delta=2.75$ eV, $U_p=3.6$ eV, and $U_d=7.9$ eV.

apart from details which can be attributed to the finite size of the cluster. The peaks 6_{Cu} and 6_O correspond to the copper and oxygen antibound states for momentum $\mathbf{q}=(0,0)$ whereas for $\mathbf{q}=(\pi,0)$ only the oxygen antibound state is visible (4_O). The peaks 3_{Cu} and 3_O are the split-off states from the mixed Cu-O two-hole band where (in contrast to Fig. 4) also the oxygen channel has significant weight. Finally, the peak 2_{Cu} is "bandlike" and corresponds to a removal state. The exact spectra show additional features not present in the BLA and TDGA. These are possibly related to processes where the two additional holes are created on initially singly occupied Cu/O atoms so that the final state has two doubly occupied sites. Such processes are neither contained in the BLA nor in the TDGA since both approximations only consider addition of hole pairs on an initially empty site. Except for these additional excitations it is apparent that for the physical parameter set the slightly better performance of the TDGA is marginal and the BLA already provides a rather good approximation.

Figure 12 shows a comparison between exact, TDGA, and BLA spectra for the half-filled cluster but with rescaled hoppings (see figure caption) to get closer to the extreme Mott limit. The exact result shows a weak feature at $\omega \approx 3.5$ eV which can be attributed to the Cu antibound state, and two peaks at higher energy which are again related to four-hole final states. In the oxygen channel this excitation acquires significant weight and the TDGA shows excellent agreement with regard to both intensity and energy of the corresponding peak. In contrast the BLA overestimates the peak intensity in the copper channel. This behavior is similar to the results in Fig. 8 and agrees with our earlier findings within the one-band model.[7]

The conclusions drawn for the half-filled cluster remain valid also for higher hole dopings. In Figs. 13 and 14 we

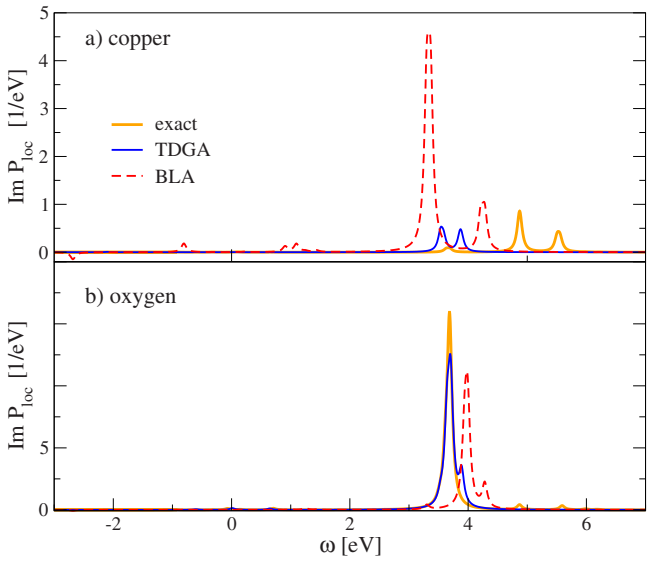

FIG. 12. (Color online) Comparison of the imaginary part of the response function for (a) copper and (b) oxygen between exact (thick solid), TDGA (thin solid), and BLA (thin dashed). The system is a half-filled ($n=1$) cluster and the spectra for oxygen(2) and oxygen(3) are identical. Parameters: $t_{pd}=0.3$ eV, $t_{pp}=-0.12$ eV, $\Delta=2.75$ eV, $U_p=3.6$ eV, and $U_d=7.9$ eV.

display the spectra for the cluster doped with four holes. In this case the lowest band of dominantly Cu character is fully occupied. In contrast to the two holes case the O_x, O_y spectra are different due to an occupancy for the oxygen(1) about a factor of two larger than for oxygen(3). This has an impact on the weight and on the energy of the respective excitations due to different local chemical potentials. For both copper

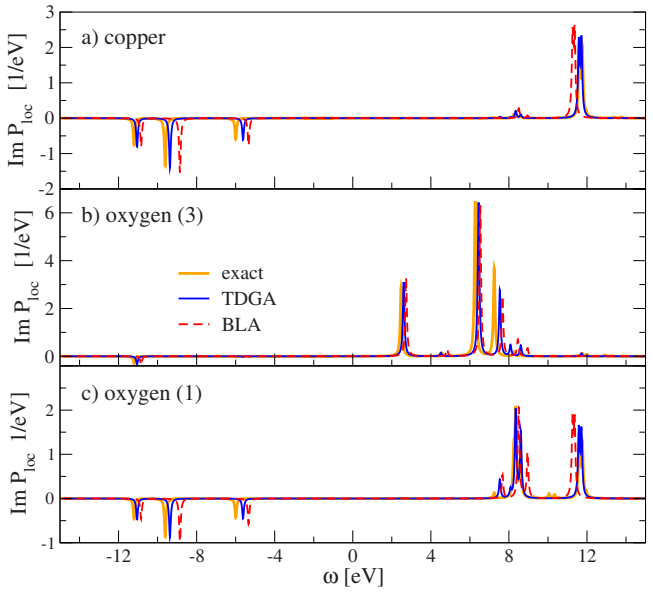

FIG. 13. (Color online) Comparison of the two-particle excitation spectra for (a) Cu, (b) oxygen on site 3, and (c) oxygen on site 1 (cf. Fig. 1) between exact (thick solid), TDGA (thin solid), and BLA (thin dashed). The cluster is doped with four holes ($N_\uparrow=N_\downarrow=2$ and filling $n=2$). Parameters: $t_{pd}=1.6$ eV, $t_{pp}=-0.6$ eV, $\Delta=2.75$ eV, $U_p=3.6$ eV, and $U_d=7.9$ eV.

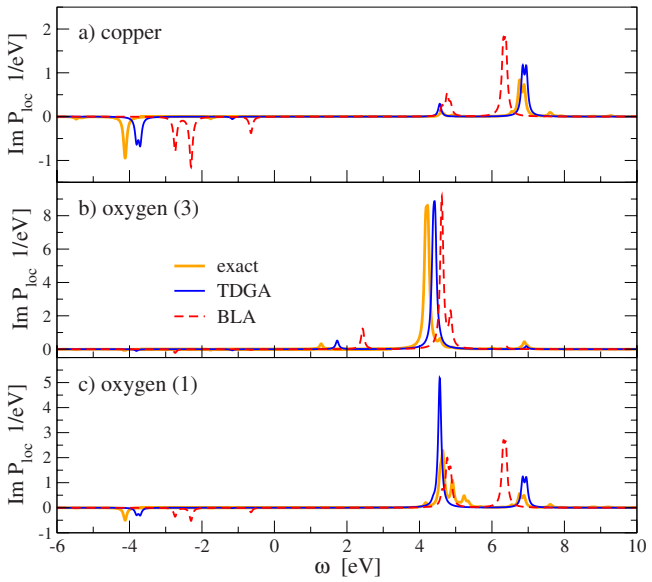

FIG. 14. (Color online) Comparison of the two-particle excitation spectra for (a) Cu, (b) oxygen on site 3, and (c) oxygen on site 1 (cf. Fig. 1) between exact (thick solid), TDGA (thin solid), and BLA (thin dashed). The cluster is doped with four holes ($N_\uparrow=N_\downarrow=2$ and $n=2$). Parameters: $t_{pd}=0.5$ eV, $t_{pp}=-0.2$ eV, $\Delta=2.75$ eV, $U_p=3.6$ eV, and $U_d=7.9$ eV.

and oxygen the spectra clearly separate in a removal part, originating from the occupied Cu band, and in an additional part, originating from states that split-off from the upper O-type band. Again we find that for the physical parameter set, Fig. 13, there are only marginal differences between the TDGA and BLA with a slightly better performance of the former. In Fig. 14 we instead show the spectra for rescaled hoppings, i.e., for stronger relative interaction. Due to the reduced hybridization between the fully occupied Cu band and the empty O-type band one may argue that the system is closer to the Cini-Sawatzky limit. The TDGA, however, still performs much better than the BLA, despite the latter actually shows a mild improvement with respect to the half-filled case.

V. CONCLUSIONS

In this paper we performed a detailed analysis of the two-hole response function for the three-band Hubbard model based on the TDGA, BLA, and exact diagonalization for a small cluster. For standard parameter sets[9,10] derived for cuprate superconductors it turns out that corrections beyond the BLA lead only to a marginal improvement of the spectra. This suggests that the correlated ground states are not in the (usually assumed) extreme Mott regime, in agreement with the conclusions of Ref. 5.

Our results indicate that a system for which the BLA performs well is not an extreme Mott insulator, i.e., the insulating phase is not solely due to local interactions. On the contrary, systems for which the more accurate TDGA performs well but the BLA does not are expected to be extreme Mott insulators. When the GA is applied to the one-band Hubbard

model, the extreme Mott insulating behavior is signaled by the Brinkman and Rice transition at $U=U_{BR}$.[41] Close and above U_{BR} the BLA fails due the lack of vertex corrections which are instead accounted for by the TDGA.[7] Here we showed that this scenario remains valid also for the, more realistic, three-band Hubbard model: the BLA agrees with the TDGA for weak to intermediate interactions but it fails in the extreme Mott regime where the TDGA still performs very well. One can question the accuracy of the GA to define the extreme Mott regime. We recall that such concept can be rigorously defined within the single-site dynamical mean-field theory (DMFT).[11] In the one-band model the value of U_{BR} is rather close to the value U_c for the metal-insulator transition estimated within DMFT. For example, for the Hubbard model on a Bethe lattice where $U_c=1.47W$,[42] with W the bandwidth one finds $U_{BR}=1.70W$. Thus U_{BR} provides the correct scale for the transition to an extreme Mott insulator and we expect that the same is true for the three-band Hubbard model.

The two-body response function $P(\omega)$ is only one of the ingredients needed to compute real Auger spectra since other relevant effects must be taken into account. To progress along this line one might embed the present framework in an approach such as, e.g., the one proposed by Cini and Drchal.[18,21] We expect that such development will stimulate further theoretical work in this sense.

Also more experimental work is needed. In fact, our results suggest to measure selective Auger processes in the copper and oxygen channels whose intensity allows for a measure of the correlation strength in cuprates. The results here obtained within the three-band model might help to assign the unrelaxed features of APECS spectra both for electron- and hole-doped cuprates. Since the antibound peaks shift significantly with respect to the chemical potential it would be very interesting to study the doping dependence. We expect that such experimental and theoretical studies, accessible to the current state of the art, will make Auger spectroscopy a much more useful tool than before, for the study of partially filled correlated systems.

ACKNOWLEDGMENTS

S. Ugenti would like to thank Francesco Guerrieri for the enlightening discussions about both Physics and Python programming. J. Lorenzana acknowledges partial financial support from MIUR, PRIN 2007 (Grant No. 2007FW3MJX003) and from the Italian Institute of Technology Seed program within the NEWDFESCM project. M. Cini and G. Stefanucci acknowledge partial financial support from MIUR, PRIN 2008AKZSXY "Spettroscopia Auger di sistemi magnetici di bassa dimensionalita:" correlazione elettronica e dicroismo."

APPENDIX: THE RESPONSE FUNCTION P^0

In this appendix we compute the response function $\hat{P}^0_{\mathbf{q}}(\omega)$ given by the single bubble diagram with Green's function relative to the mean-field GA or HF Hamiltonian $H_{\mathrm{MF}}=H_{\mathrm{GA}},H_{\mathrm{HF}}$. In the localized atomic-orbitals representation, $\{d_{x^2-y^2},p_x,p_y\}$ we write

$$H_{\mathrm{MF}}=\sum_{\mathbf{k}\sigma} C^\dagger_{\mathbf{k}\sigma}\hat{H}_{\mathbf{k}}C_{\mathbf{k}\sigma}, \tag{A1}$$

where $\mathbf{k}=(k_x,k_y)$, $C^\dagger_{\mathbf{k}\sigma}=(c^\dagger_{d,\mathbf{k}\sigma},c^\dagger_{p_x,\mathbf{k}\sigma},c^\dagger_{p_y,\mathbf{k}\sigma})$ and

$$\hat{H}_{\mathbf{k}}=\begin{pmatrix} \varepsilon_d+\Sigma_d & 2t_{pd}z_pz_d a_{\mathbf{k}} & 2t_{pd}z_pz_d b_{\mathbf{k}} \\ 2t_{pd}z_pz_d a_{\mathbf{k}} & \varepsilon_p+\Sigma_p & -4t_{pp}z_p^2 a_{\mathbf{k}}b_{\mathbf{k}} \\ 2t_{pd}z_pz_d b_{\mathbf{k}} & -4t_{pp}z_p^2 a_{\mathbf{k}}b_{\mathbf{k}} & \varepsilon_p+\Sigma_p \end{pmatrix} \tag{A2}$$

with $a_{\mathbf{k}}=\cos(k_x/2)$ and $b_{\mathbf{k}}=\cos(k_y/2)$. For $H_{\mathrm{MF}}=H_{\mathrm{GA}}$ we have $\Sigma=\Sigma^{\mathrm{GA}}$, see Eq. (20), and the z factors given in Eq. (16), while for $H_{\mathrm{MF}}=H_{\mathrm{HF}}$ we have $\Sigma=\Sigma^{\mathrm{HF}}$, see Eq. (13), and the z factors equal 1.

The matrix elements $P^{0,\alpha\beta}_{\mathbf{q}}(\omega)$ of the response function are given by the formula below,

$$P^{0,\alpha\beta}_{\mathbf{q}}(\omega)=\frac{1}{i}\int dt e^{i\omega t}\frac{1}{\Omega}\sum_{\mathbf{k}}\langle\Phi^{(0)}_N|\mathcal{T}\{c_{\alpha,\mathbf{k}+\mathbf{q}\uparrow}(t)c_{\alpha,-\mathbf{k}\downarrow}(t)c^\dagger_{\beta,-\mathbf{k}\downarrow}(0)c^\dagger_{\beta,\mathbf{k}+\mathbf{q}\uparrow}(0)\}|\Phi^{(0)}_N\rangle, \tag{A3}$$

where Ω is the number of unit cells and the operators are in the Heisenberg picture with respect to H_{MF}. Let $\hat{\mathcal{U}}_{\mathbf{k}}$ be the unitary matrix that diagonalizes $\hat{H}_{\mathbf{k}}$, i.e., $\hat{\mathcal{U}}^\dagger_{\mathbf{k}}\hat{H}_{\mathbf{k}}\hat{\mathcal{U}}_{\mathbf{k}}=\mathrm{diag}(\varepsilon^{(1)}_{\mathbf{k}},\varepsilon^{(2)}_{\mathbf{k}},\varepsilon^{(3)}_{\mathbf{k}})$. In terms of the transformed operators $\tilde{c}_{n,\mathbf{k}\sigma}=\Sigma_\alpha(\hat{\mathcal{U}}^\dagger_{\mathbf{k}})_{n\alpha}c_{\alpha,\mathbf{k}\sigma}$ the mean-field Hamiltonian reads $H_{\mathrm{MF}}=\Sigma_{n\mathbf{k}\sigma}\varepsilon^{(n)}_{\mathbf{k}}\tilde{c}^\dagger_{n,\mathbf{k}\sigma}\tilde{c}_{n,\mathbf{k}\sigma}$. Then $c_{\alpha,\mathbf{k}\sigma}(t)=\Sigma_n(\hat{\mathcal{U}}_{\mathbf{k}})\tilde{c}_{n,\mathbf{k}\sigma}e^{-i\varepsilon^{(n)}_{\mathbf{k}}t}$ and upon substitution in Eq. (A3) we find

$$\begin{aligned}P^{0,\alpha\beta}_{\mathbf{q}}(\omega)=\frac{1}{i}\int dt e^{i(\omega-\varepsilon^{(n)}_{\mathbf{k}+\mathbf{q}}-\varepsilon^{(m)}_{-\mathbf{k}})t}\frac{1}{\Omega}\sum_{\mathbf{k}}\sum_{nmrs}(\hat{\mathcal{U}}_{\mathbf{k}+\mathbf{q}})_{\alpha n}(\hat{\mathcal{U}}_{-\mathbf{k}})_{\alpha m}(\hat{\mathcal{U}}^\dagger_{-\mathbf{k}})_{\beta r}(\hat{\mathcal{U}}^\dagger_{\mathbf{k}+\mathbf{q}})_{\beta s}\\ \times[\theta(t)\langle\Phi^{(0)}_N|\tilde{c}_{n,\mathbf{k}+\mathbf{q}\uparrow}\tilde{c}_{m,-\mathbf{k}\downarrow}\tilde{c}^\dagger_{r,-\mathbf{k}\downarrow}\tilde{c}^\dagger_{s,\mathbf{k}+\mathbf{q}\uparrow}|\Phi^{(0)}_N\rangle+\theta(-t)\langle\Phi^{(0)}_N|\tilde{c}^\dagger_{r,-\mathbf{k}\downarrow}\tilde{c}^\dagger_{s,\mathbf{k}+\mathbf{q}\uparrow}\tilde{c}_{n,\mathbf{k}+\mathbf{q}\uparrow}\tilde{c}_{m,-\mathbf{k}\downarrow}|\Phi^{(0)}_N\rangle].\end{aligned} \tag{A4}$$

Performing the integral over time and taking into account that the first average in the square bracket is $\delta_{mr}\delta_{sn}[1-\theta(E_{\mathrm{F}}-\varepsilon^{(n)}_{\mathbf{k}+\mathbf{q}})][1-\theta(E_{\mathrm{F}}-\varepsilon^{(m)}_{-\mathbf{k}})]$ while the second one is $\delta_{mr}\delta_{sn}\theta(E_{\mathrm{F}}-\varepsilon^{(n)}_{\mathbf{k}+\mathbf{q}})\theta(E_{\mathrm{F}}-\varepsilon^{(m)}_{-\mathbf{k}})$ it is straightforward to obtain the final expression,

$$P^{0,\alpha\beta}_{\mathbf{q}}(\omega)=\frac{1}{\Omega}\sum_{\mathbf{k}}\sum_{nm}(\hat{\mathcal{U}}_{\mathbf{k}+\mathbf{q}})_{\alpha n}(\hat{\mathcal{U}}_{-\mathbf{k}})_{\alpha m}(\hat{\mathcal{U}}^\dagger_{-\mathbf{k}})_{\beta m}(\hat{\mathcal{U}}^\dagger_{\mathbf{k}+\mathbf{q}})_{\beta n}\frac{1-\theta(E_{\mathrm{F}}-\varepsilon^{(n)}_{\mathbf{k}+\mathbf{q}})-\theta(E_{\mathrm{F}}-\varepsilon^{(m)}_{-\mathbf{k}})}{\omega-\varepsilon^{(n)}_{\mathbf{k}+\mathbf{q}}-\varepsilon^{(m)}_{-\mathbf{k}}+i\eta\,\mathrm{sign}(\varepsilon^{(n)}_{\mathbf{k}+\mathbf{q}}+\varepsilon^{(m)}_{-\mathbf{k}}-2E_{\mathrm{F}})}. \tag{A5}$$

[1] See, for instance, E. N. Economu, *Green's Functions In Quantum Physics* (Springer, Berlin, 1979); M. Cini, *Topics and Methods in Condensed-Matter Theory* (Springer-Verlag, Berlin, 2007).
[2] M. Cini, Solid State Commun. **20**, 605 (1976); **24**, 681 (1977).
[3] G. A. Sawatzky, Phys. Rev. Lett. **39**, 504 (1977).
[4] According to the Zaanen-Sawatzky-Allen scheme for ligand metal oxides the term Mott-Hubbard insulator is reserved to the correlated insulators which satisfy that the charge gap is determined by the strong local correlations on Cu ($U_d < \Delta$) while systems as the cuprates which satisfy that $U_d > \Delta$ are termed charge-transfer insulators. Here we call both Mott insulators in the sense of a correlated insulator with even band filling.
[5] A. Comanac, L. de' Medici, M. Capone, and A. J. Millis, Nat. Phys. **4**, 287 (2008).
[6] M. Cini and C. Verdozzi, Nuovo Cimento **9**, 1 (1987).
[7] G. Seibold, F. Becca, and J. Lorenzana, Phys. Rev. Lett. **100**, 016405 (2008).
[8] G. Seibold, F. Becca, and J. Lorenzana, Phys. Rev. B **78**, 045114 (2008).
[9] A. K. McMahan, J. F. Annett, and R. M. Martin, Phys. Rev. B **42**, 6268 (1990).
[10] M. S. Hybertsen, E. B. Stechel, W. M. C. Foulkes, and M. Schlüter, Phys. Rev. B **45**, 10032 (1992).
[11] Capone and Millis notice that a system which becomes insulator when treated with single-site dynamical mean-field theory without allowing for magnetic order provides a rigorous definition of a correlated insulator due to only local interactions. M. Capone (private communication).
[12] C. A. Balseiro, M. Avignon, A. G. Rojo, and B. Alascio, Phys. Rev. Lett. **62**, 2624 (1989).
[13] J. J. Lander, Phys. Rev. **91**, 1382 (1953).
[14] C. Verdozzi, M. Cini, J. F. McGilp, G. Mondio, D. Norman, J. A. Evans, A. D. Laine, P. S. Fowles, L. Duò, and P. Weightman, Phys. Rev. B **43**, 9550 (1991).
[15] R. J. Cole, C. Verdozzi, M. Cini, and P. Weightman, Phys. Rev. B **49**, 13329 (1994).
[16] C. Verdozzi, M. Cini, and A. Marini, J. Electron Spectrosc. Relat. Phenom. **117-118**, 41 (2001).
[17] G. Fratesi, M. I. Trioni, G. P. Brivio, S. Ugenti, E. Perfetto, and M. Cini, Phys. Rev. B **78**, 205111 (2008).
[18] M. Cini and V. Drchal, J. Electron Spectrosc. Relat. Phenom. **72**, 151 (1995).
[19] O. Gunnarsson and K. Schönhammer, Phys. Rev. B **22**, 3710 (1980).
[20] E. Perfetto, Phys. Rev. B **77**, 115401 (2008).
[21] V. Drchal and M. Cini, J. Phys.: Condens. Matter **6**, 8549 (1994).
[22] For a recent review see G. Stefani, R. Gotter, A. Ruocco, F. Offi, F. Da Pieve, S. Iacobucci, A. Morgante, A. Verdini, A. Liscio, H. Yao, and R. A. Bartynski, J. Electron Spectrosc. Relat. Phenom. **141**, 149 (2004).
[23] S. M. Thurgate, Aust. J. Phys. **50**, 745 (1997).
[24] M. Cini, Surf. Sci. **87**, 483 (1979).
[25] M. Cini and C. Verdozzi, J. Phys.: Condens. Matter **1**, 7457 (1989).
[26] M. Cini and C. Verdozzi, *Auger Spectroscopy and Electronic Structure*, Springer Series in Surface Sciences Vol. 18, edited by G. Cubiotti, G. Mondio, and K. Wandelt (Springer-Verlag, Berlin, 1989), p. 122.
[27] V. Galitzki, Sov. Phys. JETP **7**, 104 (1958).
[28] J. R. Schrieffer and D. C. Mattis, Phys. Rev. **140**, A1412 (1965).
[29] Y. M. Vilk and A.-M. S. Tremblay, J. Phys. I **7**, 1309 (1997).
[30] D. van der Marel, J. van Elp, G. A. Sawatzky, and D. Heitmann, Phys. Rev. B **37**, 5136 (1988).
[31] A. Balzarotti, M. De Crescenzi, N. Motta, F. Patella, and A. Sgarlata, Phys. Rev. B **38**, 6461 (1988).
[32] R. Bar-Deroma, J. Felsteiner, R. Brener, J. Ashkenazi, and D. van der Marel, Phys. Rev. B **45**, 2361 (1992).
[33] M. C. Gutzwiller, Phys. Rev. **137**, A1726 (1965).
[34] G. Seibold and J. Lorenzana, Phys. Rev. Lett. **86**, 2605 (2001).
[35] G. Seibold, F. Becca, and J. Lorenzana, Phys. Rev. B **67**, 085108 (2003).
[36] J. P. Blaizot and G. Ripka, *Quantum Theory of Finite Systems* (MIT Press, Cambridge, Massachusetts, 1986).
[37] J. O. Sofo and C. A. Balseiro, Phys. Rev. B **45**, 377 (1992).
[38] G. Kotliar and A. E. Ruckenstein, Phys. Rev. Lett. **57**, 1362 (1986).
[39] F. Gebhard, Phys. Rev. B **41**, 9452 (1990).
[40] D. Vollhardt, Rev. Mod. Phys. **56**, 99 (1984).
[41] W. F. Brinkman and T. M. Rice, Phys. Rev. B **2**, 4302 (1970).
[42] R. Bulla, Phys. Rev. Lett. **83**, 136 (1999).